# Self-balancing Robot Modeling and Control Using Two Degree of Freedom PID Controller

Ahmad Taher Azar[1,2(✉)], Hossam Hassan Ammar[2], Mohamed Hesham Barakat[2], Mahmood Abdallah Saleh[2], and Mohamed Abdallah Abdelwahed[2]

[1] Faculty of Computers and Information, Benha University, Benha, Egypt
ahmad_t_azar@ieee.org

[2] School of Engineering and Applied Sciences, Nile University Campus, Sheikh Zayed District, Juhayna Square, 6th of October City, Giza 12588, Egypt
{hhassan, mhesham, mabdullah, moabdullah}@nu.edu.eg

**Abstract.** This paper represents the control of a two-wheel self-balancing robot based on the theory of controlling the inverted pendulum. This paper dividing the system modeling into two main parts. The first part is the dc motor and the second part are the whole mechanical design and its characteristics as a function in the motor speed and the torque depending on the system, creating two control closed loops inner and outer. The study uses conventional proportional–integral–derivative (PID) and two degree of freedom PID controllers to obtain a robust controller for the system. The inner loop controls the motor speed use the motor speed feedback signal from the encoder. The outer loop keeps the robot always in the accepted vertical angle boundary, using a six-degree of freedom gyroscope and accelerometer as a feedback signal. A state space model is obtained considering some assumptions and simplifications. The results are verified through simulations and experiments. Numerical simulation results indicate that the 2-DOF PID controller is superior to the traditional PID controller.

**Keywords:** Self-balancing robot · Segway · Inverted pendulum
Two-degree of freedom PID controller

## 1 Introduction and the Related Work

The self-balancing robot is an important device as a base to many applications in practical life like some of mobile robots. This type of robots has an enormous diversity in shape and applications. This paper represents the concept of controlling this unstable, nonlinear system. The inverted pendulum is an interesting point to have a good understanding of this problem [1, 2].

The robot structure is consisting of three horizontal layers are spaced in the vertical direction for mounting the control components [3]. In the lower face of the lower layer the motors are mounted at the upper face the inertial measurement unit (IMU), the component which is responsible for measuring the acceleration and the inclination in the three directions. At the second layer the controller and at the upper layer the driving batteries are mounted respectively [4]. The used controller is Arduino mega which is

© Springer Nature Switzerland AG 2019
A. E. Hassanien et al. (Eds.): AISI 2018, AISC 845, pp. 64–76, 2019.
https://doi.org/10.1007/978-3-319-99010-1_6

cheaper and easy to control driving a dc geared motors with built in encoders and motor drive unit as an interface between the two voltage levels control and drive motors.

One of the most important problems is to obtain a good transfer function for the motor. Obtaining the proper PID parameters and set them into the controller with fine tuning [4]. The second approach is using the two degree of freedom PID controller which could attain a higher performance than the one degree of freedom.

This paper is organized as follows: In Sect. 2, dynamical modeling of self-balancing robot is introduced. Section 3 describes the design and structure of two degree of freedom PID controllers. In Sect. 4, simulation results of control methods are presented and discussed. Finally, in Sect. 5, concluding remarks are given.

## 2 Dynamical Modeling of Self-balancing Robot

The objective of a self-balancing robot is to maintain it always stand on two wheels with changing in the horizontal position and oscillations keeping it always vertically [5].

The robot could be modeled through two sub systems first of them is inverted pendulum system and the other one is DC motor that supply the inverted pendulum with the sufficient force/torque to maintain its position as shown in Fig. 1.

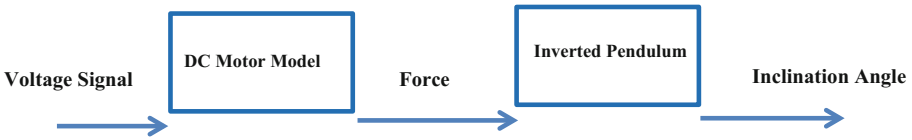


**Fig. 1.** Self-balancing robot model including the two subsystem needed

### 2.1 Dynamical Modeling of Inverted Pendulum

Figure 2 illustrates the theoretical mathematical model for an inverted pendulum on a moving carriage. Free body diagram is used here to obtain the dynamic equations of motion [6]. The self-balancing robot can be represented as an inverted pendulum on a moving carriage where the pendulum has a mass of m at a distance L from the pivot point, and an inclination angle θ from the vertical, an acceleration of $\ddot{x}$.The carriage has a mass M and external applied force of F [7]. Inverted pendulum physical parameters are summarized in Table 1.

The free-body diagrams of the two elements of the inverted pendulum system [8] is shown in Fig. 3. The forces in the free-body diagram of the carriage in the horizontal direction generates the equation of motion (1) and the forces of the pendulum in the horizontal direction generates the following equation of motion (2).

$$M\ddot{x} + b\dot{x} + N = F \tag{1}$$

$$N = m\ddot{x} + ml\ddot{\theta}\cos\theta - ml\dot{\theta}^2\sin\theta \tag{2}$$

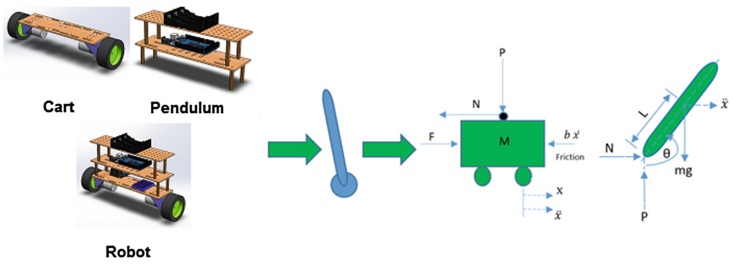


**Fig. 2.** The two-wheel self-balancing robot model as an inverted pendulum on a moving carriage

**Table 1.** Inverted pendulum physical parameters

| Symbol | Parameter |
|---|---|
| M | Cart mass |
| m | Pendulum mass |
| b | Cart Friction |
| l | Length to pendulum center of mass |
| I | Pendulum Inertia |
| F | Force applied to the cart |
| N, P | Reaction forces |
| x | Cart position coordinate |
| θ | Pendulum angle from vertical |

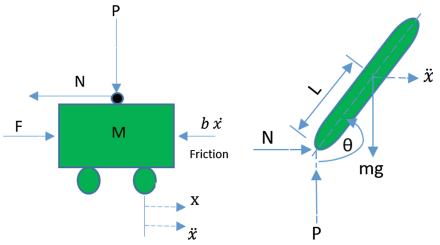


**Fig. 3.** Inverted pendulum free body diagram

Substituting (1) in (2) gives one of the two governing equations for this system:

$$(M+m)\ddot{x}+b\,\dot{x}+ml\,\ddot{\theta}\cos\theta-ml\dot{\theta}^2\sin\theta=F \tag{3}$$

Summing the forces along the axis perpendicular to the pendulum generates the Eq. (4)

$$P\,sin\,\theta+N\cos\theta-mg\sin\theta=ml\ddot{\theta}+m\ddot{x}\,\ddot{\theta}\cos\theta \tag{4}$$

Summing the moments about the centroid of the pendulum generates Eq. (5), combining (4) and (5) getting (6)

$$-Pl\,sin\theta - Nl\cos\theta = I\ddot{\theta} \tag{5}$$

$$\left(I + ml^2\right)\ddot{\theta} + mgl\sin\theta = -ml\ddot{x}\cos\theta \tag{6}$$

This set of equations needs to be linearized so as to be used in the linear control system techniques, so the equations will be linearized around the vertical upward equilibrium position, where θ = π, assuming that the system stays within a small neighborhood of this equilibrium. Let ø represent the deviation of the pendulum's position from equilibrium, where θ = π + ø, small angle approximation can be used in the nonlinear functions in the system equations:

$$cos\,\theta = \cos(\pi + \varnothing) \approx -1 \tag{7}$$

$$sin\,\theta = \sin\,(\pi + \varnothing) \approx -\varnothing \tag{8}$$

$$\dot{\theta}^2 = \dot{\varnothing}^2 \approx 0 \tag{9}$$

Substituting (7), (8) and (9) into (3) and (6) getting Eqs. (10) and (11) noting that u substituted for the input F.

$$\left(I + ml^2\right)\ddot{\varnothing} - mgl\,\varnothing = ml\ddot{x} \tag{10}$$

$$(M + m)\ddot{x} + b\,\dot{x} - ml\ddot{\varnothing} = u \tag{11}$$

**Transfer Function generation**

Taking the Laplace transform of the system equations assuming zero initial conditions to obtain the transfer functions of the linearized system equations, resulting Eqs. (12) and (13) [9].

$$\left(I + ml^2\right)\varnothing(\mathrm{s})s^2 - mgl\,\varnothing(\mathrm{s}) = ml\mathrm{X}(\mathrm{s})s^2 \tag{12}$$

$$(M + m)X(\mathrm{s})s^2 + b\,\mathrm{X}(\mathrm{s})s^2 - ml\varnothing(\mathrm{s})s^2 = U(s) \tag{13}$$

Obtaining a transfer function between the output ø and the input U(s) by eliminating the X(s) from Eqs. (12) and (13) as the transfer function only represents the relationship between a single input and a single output at a time, this yields Eq. (14).

$$X(s) = \left[\frac{I + ml^2}{ml} - \frac{g}{s^2}\right]\varnothing(s) \tag{14}$$

Substituting (14) into (13) gives (15).

$$(M+m)\left[\frac{I+ml^2}{ml}-\frac{g}{s^2}\right]\varnothing(s)s^2+b\left[\frac{I+ml^2}{ml}-\frac{g}{s^2}\right]\varnothing(s)s-ml\,\varnothing(s)s^2=U(s) \quad (15)$$

Rearranging (15) yields (16).

$$\frac{\varnothing(s)}{U(s)}=\frac{\frac{ml}{q}s^2}{s^4+\frac{b(I+ml^2)}{q}s^3-\frac{(M+m)mgl}{q}s^2-\frac{bmgl}{q}s} \quad (16)$$

Whereas,

$$q=\left[(M+m)\left(I+ml^2\right)-(ml)^2\right] \quad (17)$$

From (16) it's observed that there is a pole and zero located at the origin, so these can be canceled, and the transfer function will be:

$$P_{pend}(s)=\frac{\varnothing(s)}{U(s)}=\frac{\frac{ml}{q}s}{s^4+\frac{b(I+ml^2)}{q}s^2-\frac{(M+m)mgl}{q}s-\frac{bmgl}{q}}\left[\frac{rad}{N}\right] \quad (18)$$

Obtaining a transfer function between the output X(s) and the input U(s) by eliminating ø from Eqs. (12) and (13) yields Eq. (19).

$$P_{cart}(s)=\frac{X(s)}{U(s)}=\frac{\frac{\left(I+ml^2\right)s^2-gml}{q}}{s^4+\frac{b(I+ml^2)}{q}s^3-\frac{(M+m)mgl}{q}s^2-\frac{bmgl}{q}s}\left[\frac{rad}{N}\right] \quad (19)$$

**State Space Model**

Representing the two transfer functions (18) and (19) in the standard matrix form since the two equations are now linear after linearizing in State-Space form after rearranging to a series of first order differential equations as follows [9]:

$$\begin{bmatrix}\dot{x}\\ \ddot{x}\\ \dot{\theta}\\ \ddot{\theta}\end{bmatrix}=\begin{bmatrix}0 & 1 & 0 & 0\\ 0 & \frac{-(I+ml^2)b}{I(M+m)+Mml^2} & \frac{m^2gl^2}{I(M+m)+Mml^2} & 0\\ 0 & 0 & 0 & 1\\ 0 & \frac{-mlb}{I(M+m)+Mml^2} & \frac{mgl(M+m)}{I(M+m)+Mml^2} & 0\end{bmatrix}\begin{bmatrix}x\\ \dot{x}\\ \theta\\ \dot{\theta}\end{bmatrix}+\begin{bmatrix}0\\ \frac{I+ml^2}{I(M+m)+Mml^2}\\ \theta\\ \frac{ml}{I(M+m)+Mml^2}\end{bmatrix}U \quad (20)$$

$$y = \begin{bmatrix} 1 & 0 & 0 & 0 \\ 0 & 0 & 1 & 0 \end{bmatrix} \begin{bmatrix} x \\ \dot{x} \\ \theta \\ \dot{\theta} \end{bmatrix} + \begin{bmatrix} 0 \\ 0 \end{bmatrix} u \tag{21}$$

As due to the cart position and the pendulum's position are part of the output, so the C matrix has 2 rows.

Using *SolidWorks*$^{TM}$ CAD program to estimate the parameters of inverted pendulum model as shown in Table 2.

**Table 2.** Inverted model estimated from CAD Model

| Symbol | Quantity |
|---|---|
| M | 0.3 kg |
| m | 0.4 kg |
| b | 0.1 N/m/sec |
| I | 0.0004 Kg.m$^2$ |
| g | 9.8 N/m$^2$ |
| L | 0.084 m |

Substituting with the robot measured quantities in the State-Space model gives the two governing Eqs. (22) and (23) as follows:

$$\frac{X(s)}{U(s)} = \frac{2.86s^2 + 5.08e^{-15}s - 292.2}{s^4 + 0.286s^3 - 204.6s^2 - 29.22s} \tag{22}$$

$$\frac{\varnothing(s)}{U(s)} = \frac{29.82s + 1.665e^{-15}}{s^3 + 0.286s^2 - 204.6s - 29.22} \tag{23}$$

Using Eq. (23) which describes the system transfer function where the force is the input and inclination angle is the output.

## 2.2 DC Motor Model and Parameters Estimation

One of the most commonly actuator used in the control system is DC motor. It directly generates rotary motion which is coupled to wheels that could provide translational motion for the robot [10, 11]. The equivalent system for DC motor which consist of equivalent electric circuit of the armature and the free-body diagram or the rotor is shown in Fig. 4. The torque generated by a DC motor is proportional to the armature current and the strength of the magnetic field. In this case the used motor is a permanent magnet DC motor. So, magnetic field is assumed to be constant and therefore the motor torque is proportional to only the armature current I by a constant factor $K_t$ as shown in the equations below.

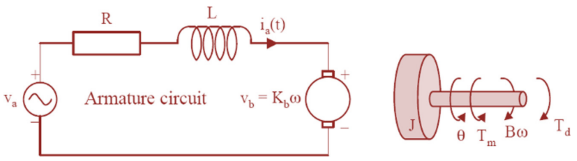


**Fig. 4.** DC motor free body diagram

The Dc Motor parameters are summarized as follows:

(J) Moment of inertia of the rotor = 0.02 kg.m$^2$
(b) Motor viscous friction constant = 0.1 N.m.s
(K) Motor torque constant and the back emf constant = 0.2
(R) Electric resistance = 2.111 Ohm
(L) Electric inductance = 0.002 H

$$T = K_t i \tag{24}$$

$$e = K_e \dot{\theta} \tag{25}$$

In SI units, Kt = Ke; therefore, K is used to represent both the motor torque constant and the electromotive force.

$$J\ddot{\theta} + b\dot{\theta} = k\, i \tag{26}$$

$$L\frac{di}{dt} + R\, i = V - K\dot{\theta} \tag{27}$$

From Eqs. (13) and (14), the Laplace transform is applied and the results are shown by the modeling equations:

$$s(Js + b)\dot{\theta}(s) = k\, I(s) \tag{28}$$

$$s(Ls + R)I(s) = V(s) - Ks\dot{\theta}(s) \tag{29}$$

$$\frac{\dot{\theta}(s)}{V(s)} = \frac{K}{(Js + b)(Ls + R) + K^2} \tag{30}$$

Similarly, for torque relation vs input voltage

$$\frac{T(s)}{V(s)} = \frac{K(s + Jb)}{(sL + R)(sJ + b) + K^2} \tag{31}$$

For the DC motor used to drive the robot, National Instrument Elvis 2 Board is used to measure the electric resistance and inductance for used motor and MATLAB system

identification tool using the given data for the DC Motor. Figure 5 illustrates the estimated DC motor rtep response versus the measured response.

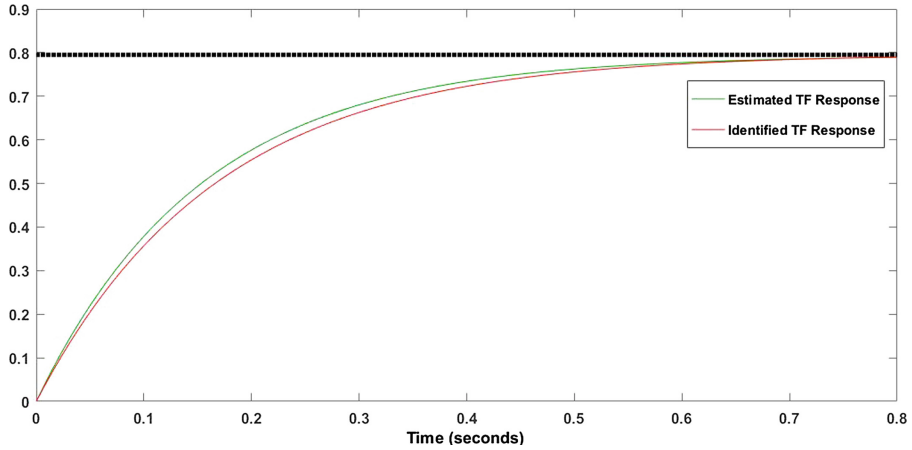


**Fig. 5.** Estimated DC motor step response vs measured response. voltage signal as an input and motor speed as an output

Finally, with substitution in Eqs. (30) and (31) to get two transfer functions one of them Speed with input voltage ad other one is torque with input voltage as following

$$G(s) = \frac{\dot{\theta}(s)}{V(s)} = \frac{0.2}{0.0422s + 0.2511} \tag{32}$$

$$P(s) = \frac{T(s)}{V(s)} = \frac{0.2s + 0.0004}{0.04222s + 0.2511} \tag{33}$$

## 3 Design of Two Degree of Freedom PID Controller

The two-degree-of-freedom (2-DOF) based controller has recently attracted the attention in different areas of control engineering community because of their better control quality for both smooth set point variable tracking and good disturbance rejection. The 2-DOF controller generates an output signal based on the difference between a reference signal and a measured system output. It computes a weighted difference signal for each of the proportional, integral, and derivative actions according to the set-point weights. The controller output is the sum of the proportional, integral, and derivative actions on the respective difference signals, where each action is weighted according to the chosen gain parameters. In general, 2DOF PID structure improves the overall closed loop performance of the process. A detailed study on various 2DOF structures are clearly presented by Araki and Taguchi [12]. In this work, the 2DOF PID

Feedforward type is used as shown in Fig. 6 where P(s) is the controlled process transfer function, $C_f$ (s) is the feedforward compensator transfer function, C(s) is the serial (or main) compensator transfer function, $r$ is the set-point, $d$ the load-disturbance, and $y$ the controlled variable. In this case, C(s) and Cf (s) are given by [12]:

$$C(s) = K_p\left\{1 + \frac{1}{T_i s} + T_D D(s)\right\} \tag{34}$$

$$C_f(s) = -K_p\{\alpha + \beta T_D D(s)\} \tag{35}$$

where α and β are controller weighting parameters ranging from 0 to 1, D(s) is the approximate derivative filter term given by:

$$D(s) = \frac{s}{1 + \tau s} \tag{36}$$

Where $\tau = T_d/K_d$

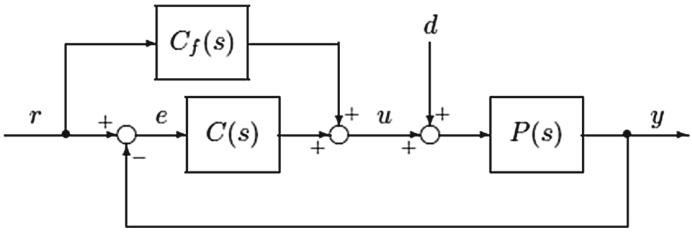


**Fig. 6.** Two-DOF PID feedforward type [12]

## 4 Simulation Results and Discussions

The performance of the controllers is analyzed based on the time domain parameters ($M_p$, $t_s$), error values like Integral of Time multiplied Absolute Error (ITAE), Integral of Squared Error (ISE), Integral of Absolute Error (IAE) and Integral of Time Multiply Squared Error (ITSE) [13, 14]. In the first phase, the conventional PID Controller is used for the self-balancing robot control as shown in Fig. 7.

In the second phase, the control of two wheeled self-balancing robot consists of two main loops as shown in Fig. 8. One of them for DC motors (inner loop control using 1-DOF PID controller) to maintain the required speed and torque for the pendulum (outer loop control using 2-DOF PID controller) which maintains the inclination angle of the robot. Each DC motor has its own PID controller and a feedback sensor where the two motors represents the inner control loop in which the speed and torque of the motors is controlled. The outer loop which control's the inclination of the two wheeled self-balancing robot consists of separate -DOF PID controller to control the inclination angle.

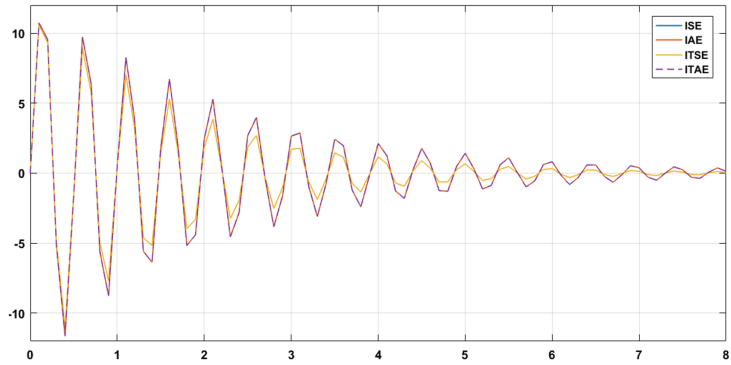


**Fig. 7.** 1 DOF PID controller for self-balancing robot control

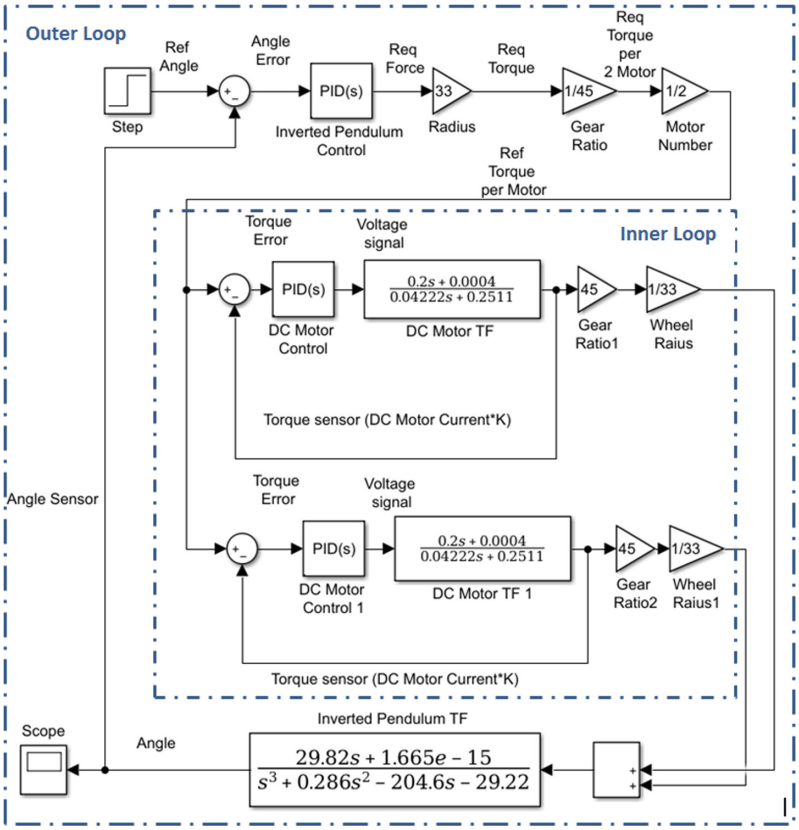


**Fig. 8.** Block diagram of 1-DOF and 2-DOF PID controller for Robot control

For the given DC motor, the step response of proportional (P), proportional-integral (PI), proportional-derivative (PD) and proportional-integral-derivative (PID) Controllers for speed and torque are compared as shown in Fig. 9. It's noted that the PID controller, in general, provides faster response and improved stability as compared to other types of controllers.

In the third phase, the control of two wheeled self-balancing robot consists of two main loops one of them for DC motor (inner loop control using 2-DOF PID controller) to maintain the required speed and torque for the pendulum. The outer loop control consists of another 2-DOF PID controller to maintain the inclination angle of the robot as shown in Fig. 10. For the given DC Motor response to 2-DOF P, PI, PD, PID controller as shown in Fig. 11. It can be concluded that 2-DOF PID controller is more

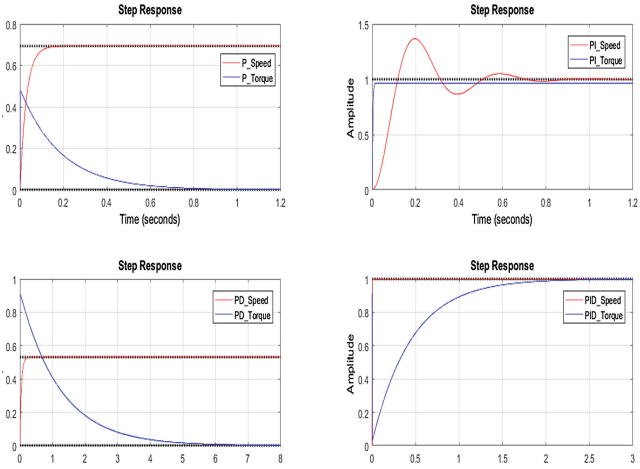


**Fig. 9.** P, PI, PD and PID controller for inner loop DC motor

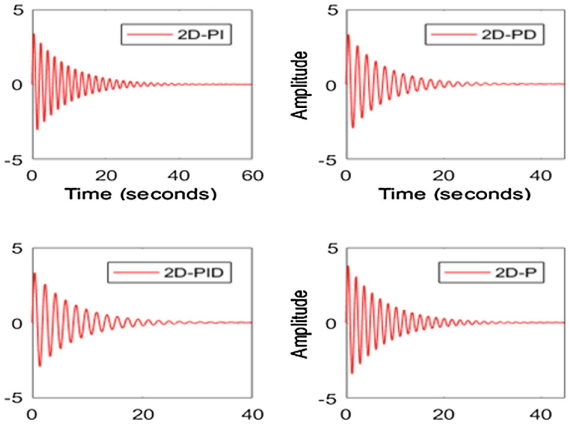


**Fig. 10.** Response of the pendulum to 2-DOF P, PI, PD, PID controllers

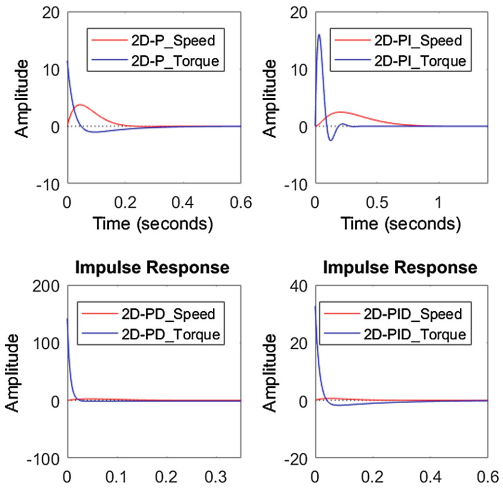


**Fig. 11.** DC motor with 2-DOF P, PI, PD, PID controller response to impulse input

effective than the traditional PID controller. The simulation results show that the setting value tracking characteristics of the system is obviously enhanced when the main controller is the two-degree-of-freedom with a feed-forward controller, compared to conventional PID controller.

## 5 Conclusion

In this paper, a model of a two-wheel self-balancing robot based on the theory of controlling the inverted pendulum is proposed. The model is obtained by two approaches, the mathematical approach and the system identification with parameter estimation approach based on experimental results. This study compares the results of two controllers conventional PID and 2-DOF PID controllers. The simulation results showed that the 2-DOF controller approach is much faster in response and disturbance rejection as well as smaller error than conventional PID controller while maintaining set-point performance.

## References

1. Azar, A.T., Serrano, F.E.: Adaptive sliding mode control of the furuta pendulum. In: Azar, A.T., Zhu, Q. (eds.) Advances and Applications in Sliding Mode Control systems. Studies in Computational Intelligence, vol. 576, pp. 1–42. Springer, Heidelberg (2015)
2. Azar, A.T., Vaidyanathan, S.: Handbook of Research on Advanced Intelligent Control Engineering and Automation. Advances in Computational Intelligence and Robotics (ACIR). IGI Global, Pennsylvania (2015). ISBN 9781466672482
3. Deng, M., Inoue, A., Sekiguchi, K., Jiang, L.: Two-wheeled mobile robot motion control in dynamic environments. Robot. Comput. Integr. Manuf. **26**(3), 268–272 (2010)

4. Bui, T.H., Nguyen, T.T., Chung, T.L., Kim, S.B.: A simple nonlinear control of a two-wheeled welding mobile robot. Int. J. Control Autom. Syst. (IJCAS) **1**(I), 35–42 (2003)
5. Kim, Y., Kim, S.H., Kwak, Y.K.: Dynamic analysis of a nonholonomic two-wheeled inverted pendulum robot. J. Intell. Robot. Syst.: Theory Appl. **44**(1), 25–46 (2005)
6. Juang, H.S., Lurrr, K.Y.: Design and control of a two-wheel self-balancing robot using the arduino microcontroller board. In: 2013 10th IEEE International Conference on Control and Automation (ICCA), 12–14 June 2013, Hangzhou, China (2013)
7. Thibodeau, B.J., Deegan, P., Grupen, R.: Static analysis of contact forces with a mobile manipulator. In: Proceedings 2006 IEEE International Conference on Robotics and Automation, 15–19 May 2006, Orlando, FL, USA, pp. 4007–4012 (2006)
8. Sun, C., Lu, T., Yuan, K.: Balance control of two-wheeled self-balancing robot based on linear quadratic regulator and neural network. In: 2013 Fourth International Conference on Intelligent Control and Information Processing (ICICIP), 9–11 June 2013, Beijing, China (2013)
9. Lin, S.C., Tsai, C.C.: Develop of a self-balancing human transportation vehicle for the teaching of feedback control. IEEE Trans. Educ. **52**(1), 157–168 (2009)
10. Sugie, T., Fujimoto, K.: Controller design for an inverted pendulum based on approximate linearization. Int. J. Robust Nonlinear Control **8**(7), 585–597 (1998)
11. Takei, T., lmamura, R., Yuta, S.: Baggage transportation and navigation by a wheel inverted pendulum mobile robot. IEEE Trans. Ind. Electr. **56**(10), 3985–3994 (2009)
12. Araki, M., Taguchi, H.: Two-degree-of-freedom PID controllers. Int. J. Control Autom. Syst. **1**(4), 401–411 (2003)
13. Sánchez, H.S., Visioli, A., Vilanova, R.: Optimal nash tuning rules for robust PID controllers. J. Franklin Inst. **354**(10), 3945–3970 (2017)
14. Azar, A.T., Serrano, F.E.: Robust IMC-PID tuning for cascade control systems with gain and phase margin specifications. Neural Comput. Appl. **25**(5), 983–995 (2014)